ACS OMEGA

Open Access

http://pubs.acs.org/journal/acsodf

Article

Influence of Fatty Acid Modification on the Anticancer Activity of the Antimicrobial Peptide Figainin 1

Zhenbin Han, Dongmei Feng, Wenxuan Wang, Yue Wang, Maosheng Cheng, Huali Yang,* and Yang Liu*

Cite This: *ACS Omega* 2023, 8, 41876−41884

Read Online

ACCESS | Metrics & More | Article Recommendations | Supporting Information

ABSTRACT: Antimicrobial peptides derived from the skin secretions of amphibians have made important progress in tumor therapy due to their unique mechanism of destroying cell membranes. Figainin 1 (F1) is an 18-amino acid antimicrobial peptide from the skin secretions of *Boana raniceps* frogs. In a previous study, F1 was shown to inhibit cancer cell proliferation. F1 is composed entirely of natural amino acids; therefore, it is easily degraded by a variety of proteases, resulting in poor stability and a short half-life. In the present study, we used a fatty acid modification strategy to improve the stability of Figainin 1. Among the 8 peptides synthesized, A-10 showed the strongest antiproliferative activity against K562 cells and the other four tumor cell lines, and its stability against serum and proteinase K was improved compared with F1. We found that A-10 works through two mechanisms, cell membrane destruction and apoptosis, and can arrest the cell cycle in the G0/G1 phase. Moreover, A-10 exhibited self-assembly behavior. Overall, it is necessary to select a fatty acid with a suitable length for modification to improve the stability and antiproliferative activity of antimicrobial peptides. This study provides a good reference for the development of antimicrobial peptides as effective anticancer compounds.

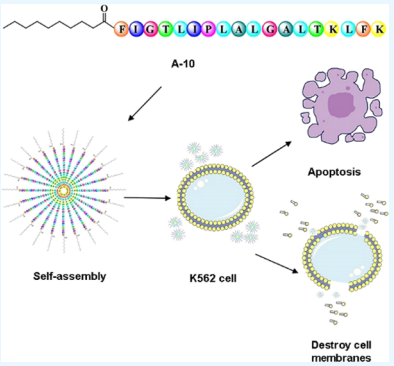

INTRODUCTION

Despite the rapid development of global medical technology, malignant tumors are still an important public health problem that threatens human health.[1] Chronic myelogenous leukemia (CML) is a hematologic malignancy, with an annual incidence of 1.0−1.5/10^5.[2] The initial clinical treatment options for CML include hydroxyurea, busulfan, and interferon-α, and the 10-year survival rate of patients is 10−20%.[3] Since BCR-ABL tyrosine kinase inhibitors have been approved for use in the clinic, the survival rate of patients with chronic myelogenous leukemia has improved significantly, and the first-generation tyrosine kinase inhibitor imatinib mesylate has become the gold standard first-line treatment.[4] Imatinib mesylate changed the treatment and prognosis of CML and served as a paradigm for the development of targeted therapies for other cancers. However, the emergence of resistance to imatinib mesylate was reported soon after, and second- and third-generation tyrosine kinase inhibitors were thus developed.[5] With the approval of second- and third-generation tyrosine kinase inhibitors, the majority of CML patients enjoy long-term remission and near-normal life expectancy. Unfortunately, some CML patients develop resistance to third-generation tyrosine kinase inhibitors, leading to treatment failure and progression to blast phase CML. Mutations in the ABL kinase domain and other domains that control the conformation of the kinase domain impede drug binding by either altering the BCR-ABL conformation or blocking binding altogether, which is the most common mechanism of resistance. Although PROTAC molecules targeting BCR-ABL have provided new treatment ideas for CML patients, the development of BCR-ABL tyrosine kinase inhibitor-resistant CML is still an urgent problem to be solved.[6]

Peptides have achieved significant success as active pharmaceutical ingredients.[7] Currently, more than 80 peptides have been approved as therapeutic drugs in the United States, Europe, and Japan. As a class of host defense peptides expressed in many species, antimicrobial peptides are potential therapeutic options in the drug arsenal due to their high permeability, specificity, and few side effects.[8] Many of these peptides were found in amphibian skin, and they are selective for cancer cells due to the higher abundance of negatively charged molecules, such as phosphatidylserine, glycoproteins, and glycolipids, on the outer plasma membrane of cancer cells.[9] The cell membranes of bacteria and cancer cells both contain a high proportion of net negative charges, and the anticancer activity of antimicrobial peptides can be exerted by the electrostatic and hydrophobic interactions between the

Received: September 7, 2023
Revised: October 3, 2023
Accepted: October 12, 2023
Published: October 27, 2023

https://doi.org/10.1021/acsomega.3c06806
ACS Omega 2023, 8, 41876−41884

Table 1. Physicochemical Properties of Peptides

name	sequence	net charge	t_R[a] (min)	molecular weight[b]	
				calculated	measured
F1	FIGTLIPLALGALTKLFK-NH_2	+3	10.59	1915.41	1915.21
A-4	butyric acid-FIGTLIPLALGALTKLFK-NH_2	+2	11.79	1984.25	1985.26
A-6	caproic acid-FIGTLIPLALGALTKLFK-NH_2	+2	11.91	2012.28	2013.29
A-8	octanoic acid-FIGTLIPLALGALTKLFK-NH_2	+2	12.15	2040.31	2041.32
A-10	decanoic acid-FIGTLIPLALGALTKLFK-NH_2	+2	12.30	2068.34	2069.35
A-12	lauric acid-FIGTLIPLALGALTKLFK-NH_2	+2	12.67	2096.37	2097.38
A-14	myristic acid-FIGTLIPLALGALTKLFK-NH_2	+2	12.81	2124.41	2125.41
A-16	palmitic acid-FIGTLIPLALGALTKLFK-NH_2	+2	12.93	2152.44	2153.44
A-18	stearic acid-FIGTLIPLALGALTKLFK-NH_2	+2	13.17	2180.47	2181.47

[a] t_R: Retention time was determined by HPLC.The HPLC condition: a linear gradient of 50−100% methanol (with 0.1% TFA) in water (with 0.1% TFA) over 20 min (50−100% for 10 min, then 100% for 10 min) on a ZORBAX C18 column, λ = 210 nm. [b]Calculated molecular weight is predicted by ChemDraw, and the measured molecular weight is determined by ESI-MS.

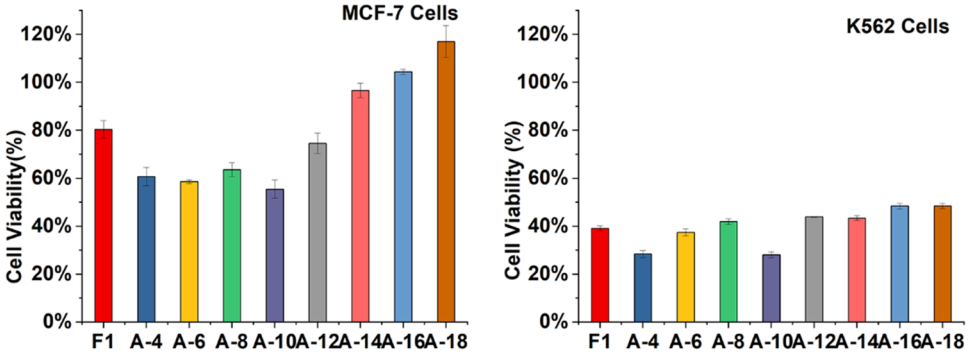

Figure 1. Cytotoxic efficiency of the peptides at 10 μM on MCF-7 cells and K562 cells.

antimicrobial peptides and the biofilm. To date, at least two antimicrobial peptides (LL-37 and LTX-315) have entered clinical trials for cancer treatment. The Peptide Database (APD, http://aps.unmc.edu/AP/) contains more than 2000 active peptides, more than 200 of which have antitumor activity.[10] The main mechanism of antimicrobial peptides is through their interaction with the cell membrane, which leads to cell membrane lysis or permeation.[11] Antimicrobial peptides are generally cationic amphiphiles with a high content of hydrophobic residues. These properties enable them to interact with negatively charged cancer cell membranes, leading to cancer cell death, and lower the risk of the development of resistance.[12] To date, three typical antimicrobial peptide membrane failure models have been proposed, including the barrel stave model, carpet model, and annular whole model.[13,14] In addition to membrane destruction, antimicrobial peptides may also have multiple other mechanisms. For example, antimicrobial peptides can inhibit tumor cell proliferation by inducing apoptosis.[15,16] Unfortunately, the instability of this peptide leads to it having poor pharmacokinetic properties.[17] Various design strategies have been developed to improve the stability of antimicrobial peptides, such as modification with unnatural amino acids, lipidation, cyclization, peptidomimetics, and nanotechnology.[18−21] Lipidation generally refers to the attachment of fatty acids to the N-terminal or Lys residues of antimicrobial peptides.[22] Lipidation can increase the stability of antimicrobial peptides by blocking the region vulnerable to proteases or forming a supramolecular structure, further prolonging the effective time of the antimicrobial peptide drug.[23,24] Lipidation is a useful modification to tune the proteolytic stability and antibacterial activity of antimicrobial peptides. Modified with various fatty acids, a series of glucagon-like peptide 1 analogues were developed to prolong their plasma half-life through albumin binding.[25]

F1 is a novel antibacterial and anticancer peptide from the skin secretion of the frog *Boana raniceps*.[26,27] F1 is a cationic peptide 18 amino acids in length that is rich in hydrophobic leucine and isoleucine residues and has an amidated C-terminus. F1 has an α-helical conformation in the presence of trifluoroethanol (TFE), and it also shows antiproliferative activity (IC_{50} values ranging from 10.5 to 13.7 μM) against cancer cells and murine fibroblasts. In this study, we synthesized eight peptides with fatty acyl chains ranging from 4 to 18 carbon atoms in length conjugated to the N-terminus of F1. We determined the antitumor activity of the 8 peptides by the Cell Counting Kit-8 (CCK-8) method. We also determined the secondary structure of the peptide and investigated its self-assembly behavior. Moreover, we investigated the interaction between the lipopeptide and the leukemia cell membrane and discussed its mechanism of action.

RESULTS

Peptide Sequences and Characteristics. In this work, we conjugated fatty acid chains of different lengths (C4, C6, C8, C10, C12, C14, and C16) to the N-terminus of F1. All peptides had a net charge of +2 at neutral pH (Table 1). The fatty acid was linked to the α-amino group of the phenylalanine of F1 via an amide bond. The correct molecular weights of F1 and the lipopeptides were confirmed by mass spectrometry. We analyzed the hydrophobicity of F1 and lipopeptides by

https://doi.org/10.1021/acsomega.3c06806
ACS Omega 2023, 8, 41876−41884

high-performance liquid chromatography (HPLC). The retention times of F1 and the lipopeptides gradually increased with increasing aliphatic chain length. The proportion of acetonitrile applied at the elution time of the lipopeptides with longer fatty acid chains was higher, and it can be preliminarily concluded that their hydrophobicity gradually increased with chain elongation.

In Vitro Anticancer Activity of the Peptides. First, the concentration of MCF-7 and K562 cells by F1 and its derivative lipopeptides at a concentration of 10 μM was determined by the CCK8 method. As shown in Figure 1, F1 and some of its derived lipopeptides exhibited inhibitory activity against two tumor cell lines after 24 h of incubation. The anticancer activity of the lipopeptide obtained with the 10 carbon atom long fatty acid was better than that of F1 when the length of the modifying fatty acid was more than 10 carbon atoms; the anticancer activity of the lipopeptide was lower than that of F1. This phenomenon was more pronounced in MCF-7 cells than in K562 cells, indicating that modification with a fatty acid 10 carbon atoms in length is crucial for enhanced activity. In MCF-7 cells, it was observed that the C12−C18 modifications decreased the anticancer activity of F1 due to the relatively slower kinetics of cell killing caused by the longer aliphatic chain. This phenomenon was also observed in K562 cells but to a lesser extent. Then, we used A-10 as the optimal compound to measure the IC50 values in five kinds of cells including MCF-7, HCT-116, K562, CCRF-CEM, and A549. As shown in Table 2, A-10 had better anticancer activity than Figainin 1 in the above five cell types.

Table 2. IC_{50} Value (μM) Detected by the CCK8 Method[a]

	IC_{50} (μM)				
compound	MCF-7	HCT-116	K562	CCRF-CEM	A549
F1	11.17	8.35	8.18	9.31	14.10
A-10	8.18	6.82	5.76	6.24	13.50

[a]Note: The experimental results are the mean of three results.

From the perspective of cell type, the inhibitory activity of A-10 on cells in suspension is stronger than that on adherent cells, suggesting that it has better activity against hematological tumor cells and poorer activity against solid tumor cells, especially lung cancer cells. Due to its anticancer activity against K562 and CCRF-CEM blood tumor cells, we finally selected K562 cells for the final test.

Anticancer Mechanism of the Peptides. Antimicrobial peptides have a special mechanism by which they inhibit the proliferation of cancer cells, which is by dissolving the cell membrane. This special mechanism endows the peptide with good anticancer activity against drug-resistant cells. Therefore, we first evaluated the activity of F1 and its derivative peptides on K562 cell membrane lysis by lactate dehydrogenase (LDH) leakage assays. As shown in Figure 2A, after 24 h of action by F1 and its derivative peptides, both F1 and A-10 destroyed cell membranes, and the activity of A-10 was stronger than that of F1. This indicates that fatty acid modification can improve the activity of F1 and explains why A-10 has stronger anticancer activity.

In addition to the mechanism of direct cell membrane disruption, antimicrobial peptides can also induce cell death by disrupting subcellular organelles (such as mitochondria, lysosomes, or the endoplasmic reticulum) and a variety of other mechanisms that work together. Different antimicrobial peptides have different mechanisms of action in different cell lines. Therefore, we used flow cytometry to detect the effects of F1 and its derivative lipopeptides on apoptosis and cycle changes in K562 cells. As shown in Figure 2B, after 24 h of treatment with F1 and its derivative lipopeptides at a concentration of 10 μM, both F1 and A-10 induced apoptosis in K562 cells. F1 increased the number of cells in late apoptosis, while A-10 increased the number of cells in early apoptosis. Overall, the number of normal cells in the F1 group was less than that in the A-10 group, indicating that F1 can induce apoptosis better than A-10. Combining these data with those from the LDH leakage test, A-10 can exert anticancer activity not only by destroying the cell membrane but also by inducing apoptosis. Fatty acid modification of F1 increases its hydrophobicity and enhances its ability to destroy cell membranes. However, apoptosis induction decreased, indicating that the increase in the anticancer activity of A-10 mainly depends on the destruction of the cell membrane.

It has been reported that antimicrobial peptides can cause cell cycle arrest. We detected the effects of Figainin 1 and its derivative lipopeptide on the K562 cell cycle by flow cytometry. As shown in Figure 3A, the proportion of cells in the G1 phase after treatment with Figainin 1 and A-10 was significantly increased compared with that in the blank group, indicating that both Figainin 1 and A-10 can arrest the cell cycle in the G0/G1 phase.

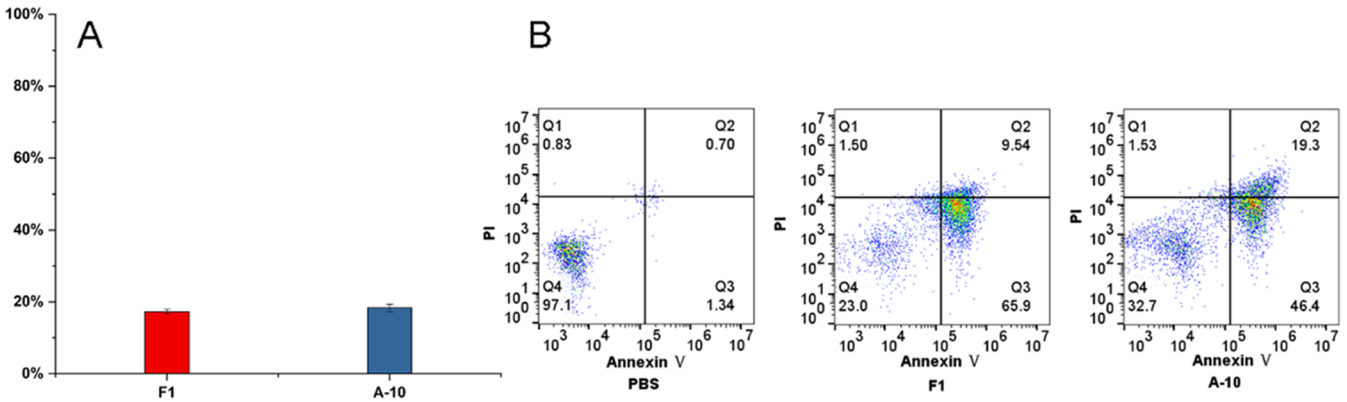

Figure 2. Mechanism of peptide inhibiting cancer cell proliferation. (A) 10 μM peptide induces 24 h LDH leakage in K562 cells. (B) Apoptosis in K562 cells induced by 10 μM peptide.

https://doi.org/10.1021/acsomega.3c06806
ACS Omega 2023, 8, 41876−41884

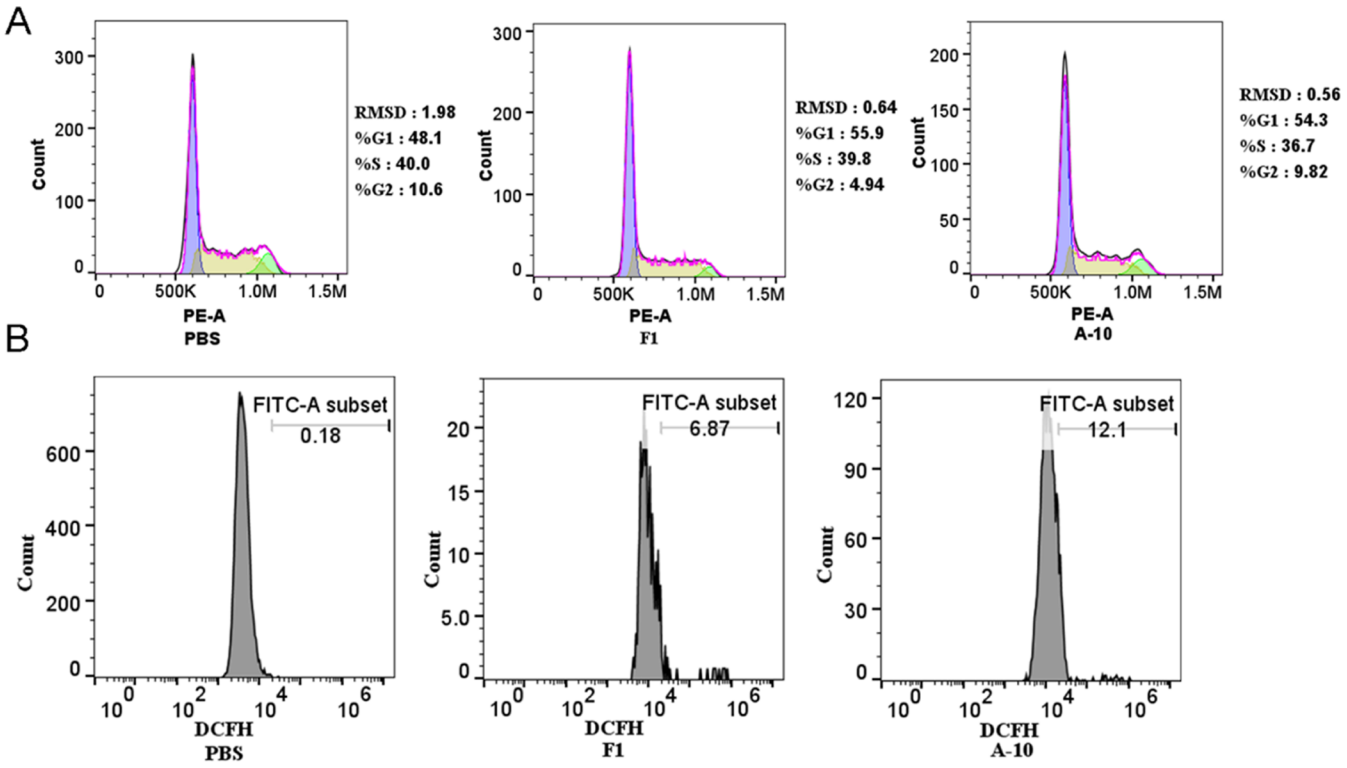

Figure 3. Detection of K562 cell cycle and ROS by flow cytometry. (A) Flow cytometry test of 10 μM peptide for 24 h on K562 cells cycle. (B) Effect of 10 μM peptide on ROS of K62 cells tested by flow cytometry for 24 h.

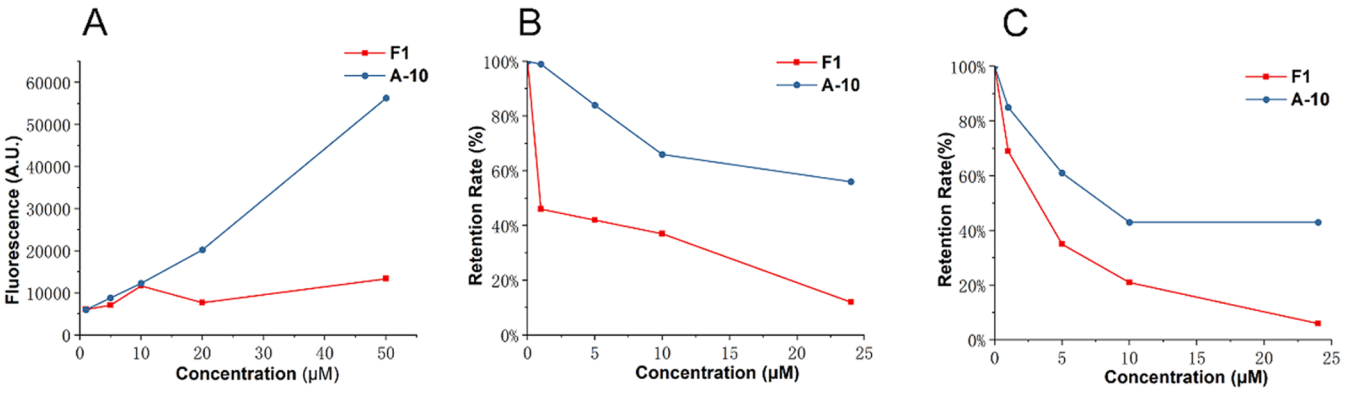

Figure 4. Peptide self-assembly test and stability test. (A) Microplate reader measures the fluorescence of ANS relative to the peptide concentration. (B) Detection of peptide stability to serum by a microplate reader. (C) Detection of peptide stability to proteinase K by a microplate reader.

It has been reported that mitochondrial damage leads to increased reactive oxygen species (ROS) production and that high levels of ROS induce G1 phase arrest, which further induces cell death. We measured the ROS levels in cells using flow cytometry. As shown in Figure 3B, after treating K562 cells with F1 and A-10 for 24 h, we observed that the fluorescence intensity in the F1 and A-10 groups increased significantly, indicating that the mitochondria in these two groups of cells produced a large amount of ROS. These phenomena indicated that F1 and A-10 caused severe mitochondrial damage. Therefore, the increased levels of ROS in K562 cells treated with F1 and its derivative lipopeptides may be the main factor leading to G0/G1 phase arrest.

Self-Assembly of the Peptides. Most antimicrobial peptides have amphiphilic structure. After modification with hydrophobic fatty acids, antimicrobial peptides usually self-assemble to form a nanostructure. These nanostructures may improve their stability and affect their cell entry mechanism. The cell membrane is composed of a phospholipid bilayer, and the hydrophobic lipopeptide fatty acid chain self-assembled into a nanostructure on the outside, which can increase the efficiency of lipopeptide passage through the cell membrane. 8-Anilino-1-naphthalenesulfonate (ANS) is a hydrophobic probe that can bind to the hydrophobic surface of self-assembling peptides, after which the fluorescence intensity increases. As shown in Figure 4A, we measured the fluorescence intensity of F1 and A-10 in ANS solution at different concentrations. It can be seen from the results that the fluorescence intensity of A-10 showed an obvious linear increase, indicating that A-10 self-assembled in solution. However, the fluorescence of F1 did not increase significantly, indicating that F1 did not self-assemble

https://doi.org/10.1021/acsomega.3c06806
ACS Omega 2023, 8, 41876−41884

in solution. Self-assembled structures have been reported to enhance the stability of peptides. To further confirm this statement, we measured the stability of F1 and its derivative lipopeptides against proteinase K and in serum. As shown in Figure 4B, after proteinase K treatment for 24 h, 43% of A-10 remained, while only 6% of Figainin 1 remained, indicating that the stability of F1 was indeed improved by fatty acid modification. We think that the self-assembly of the lipopeptide makes monomer release difficult, and the self-assembled structure can mask the cleavage site of proteinase K. We also determined the stability of F1 and its lipopeptide in 10% serum, as shown in Figure 4C. The stability of A-10 in serum was similar to that in proteinase K. After treatment with 10% serum for 24 h, 56% of A-10 remained, while only 12% of F1 remained. This result shows that fatty acid modification can increase not only the proteinase K stability of A-10 but also the serum stability of A-10. Overall, fatty acid modification improved the proteinase K and serum stability of the peptide, thus achieving the goal of our design.

DISCUSSION

The antimicrobial peptides secreted from the skins of amphibians have various functions, such as antibacterial and antitumor activities, but they still have disadvantages, such as poor stability. To improve the stability of these peptides, a variety of strategies have been reported in the literature, including stapling, cyclization, unnatural amino acid substitution, and fatty acid modification.[28,29] However, these strategies do not always work. Some modification strategies cannot improve the stability of the peptide, and some will lead to a decrease in the biological activity.[30,31] Therefore, it is necessary to screen modifications to the leading peptide. In this study, we selected fatty acids with carbon chain lengths of 4, 6, 8, 10, 12, 14, 16, and 18 to modify lead peptide F1.

Although antimicrobial peptides have antibacterial and antitumor activities, most cannot penetrate cell membranes.[32] The cell membrane is a phospholipid bilayer. By increasing the hydrophobicity of a peptide, it is possible to increase the efficiency of its passage through the cell membrane and improve its activity.[33] By comparing the HPLC retention times of F1 and its derivative lipopeptides, we found that the hydrophobicity increased with increasing fatty acid chain length from A-4 to A-18.

The effect of fatty acid modification on the anticancer activity of a peptide is crucial; therefore, we first detected the anticancer activity of F1 and its derivative lipopeptides. It has been reported that the IC_{50} value of F1 in Hela, MCF-7 and B16F10 cells is approximately 10 μM; therefore, we chose 10 μM as the initial screening concentration. We chose adherent MCF-7 and suspended K562 cells for detection. According to the preliminary screening results, modification with C4, C6, C8, and C10 fatty acids led to an increase in the activity of F1 in MCF-7 and K562 cells and A-10 displayed the strongest anticancer activity.

However, the C12, C14, C16, and C18 fatty acid modifications decreased the anticancer activity of F1. We think that hydrophobic fatty acid modification will indeed improve the anticancer activity of antimicrobial peptides, but the C4, C6, and C8 fatty acid carbon chains are too short to form a self-assembled structure; instead, their increased activity is simply due to the increased hydrophobicity. Lipopeptides can self-assemble after the C10 fatty acid modification, which was also verified in our subsequent experiments. After F1 was incubated with the hydrophobic probe ANS, we did not detect an obvious increase in fluorescence intensity, while A-10 produced a notable enhancement in fluorescence intensity after incubation with the probe, proving that A-10 did indeed form a self-assembled structure. Therefore, the self-assembled structure that formed after the C10 fatty acid modification enhanced the ability of the peptide to be taken up by cells. However, A-10 has a loose structure and can easily release monomers upon cell entry. This led to the strongest anticancer activity of A-10. With further elongation of the carbon chain with C12, C14, C16, and C18 fatty acid modifications, the lipopeptides gradually formed stable self-assembled structures and could not release monomers quickly. This results in these lipopeptides having slower cell killing kinetics, making A-10 less active than F1 against cancer cells after 24 h. The anticancer activity of A-10 was stronger against cells in suspension than against adherent cells. We further determined the IC_{50} value of A-10 in five kinds of cells. Among adherent cells, A-10 displayed strong anticancer activity against colon cancer and breast cancer cells but poor anticancer activity against lung cancer cells.

To verify the presumed reason for the enhanced anticancer activity of A-10, we conducted a preliminary mechanistic study. First, we used flow cytometry to detect cell apoptosis induced by F1 and its derivative lipopeptides. Both F1 and A-10 induced apoptosis. Most of the K562 cells treated with F1 were apoptotic, and the proportion in late apoptosis was greater than that in early apoptosis. Compared with F1, A-10 treatment reduced the proportion of apoptotic K562 cells, and the proportion in early apoptosis was higher than that of late apoptotic cells.

Destruction of the cell membrane will lead to the release of cytoplasmic enzymes into the culture medium, including LDH, which has relatively stable enzyme activity.[34] By detecting the activity of the LDH released from cells into the culture medium, the extent of cell membrane damage can be analyzed.[35] One of the most common mechanisms by which antimicrobial peptides operate is the disruption of the cell membrane. Antimicrobial peptides can destroy the integrity of cancer cell membranes by interacting with the phospholipid molecules present. This causes leakage of intracellular substances, which eventually leads to cell death. LDH leakage is regarded as an important indicator of cell membrane integrity and is widely used in cytotoxicity assays.[36] We performed LDH leakage experiments with F1 and its derived lipopeptides. Both F1 and A-10 damaged the cell membrane and caused leakage of cell contents and cancer cell death. After 24 h, A-10 showed produced more LDH leakage. This result shows that fatty acid modification leads to better disruption of the cell membrane, possibly because fatty acid modification increases the hydrophobicity and allows a loose self-assembled structure to form.

Antimicrobial peptides have been reported to cause cell cycle arrest.[37−39] We thus performed cell cycle detection after treatment with F1 and its derived lipopeptides using flow cytometry. F1 and A-10 caused significant arrest of the cells in the G0/G1 phase.

It has been reported that high levels of ROS induce G1 arrest.[40] When cells are stimulated, the level of ROS will increase sharply, which may cause DNA damage, inhibit gene expression, cause protein misfolding, and even affect protein synthesis, causing serious damage to the cell structure. When ROS levels exceed the capacity of endogenous antioxidant

https://doi.org/10.1021/acsomega.3c06806
ACS Omega 2023, 8, 41876−41884

defenses, the redox balance will be disrupted, causing changes in the structures of DNA, lipids, and proteins, eventually leading to cell death.[41] Mitochondrial damage leads to increased ROS generation, which further induces cell death. Therefore, we assessed mitochondrial function by measuring changes in the ROS levels. After 24 h, F1 and A-10 enhanced ROS production in the mitochondria. Of note, A-10 induced more ROS production, indicating severe mitochondrial damage.

To verify whether fatty acid modification improves peptide stability, we tested the serum stability and proteinase K stability of F1 and its derived lipopeptides. Due to the strong positive charge of cationic drugs, these compounds adsorb proteins in serum and cause drug inactivation. After incubation in 10% serum for 1 h, 54% of F1 was rapidly degraded, while A-10 modified fatty acids were hardly degraded. The degradation trends of F1 and A-10 were similar. After 24 h of incubation, only 12% of F1 remained, while 56% of A-10 remained, which indicated that fatty acid modification is an effective strategy to improve peptide stability.

Proteinase K is a serine protease with efficient enzymatic activity and broad substrate specificity.[42] It preferentially cleaves ester and peptide bonds adjacent to the C-terminus of hydrophobic amino acids, sulfur-containing amino acids, and aromatic amino acids. Proteinase K is commonly used to test the stability of peptides. We examined the stability of F1 and A-10 after incubation with proteinase K, and A-10 had better proteinase K resistance than F1. After incubation for 24 h, only 6% of F1 remained, while 43% of A-10 remained. Fatty acid modification was thus shown to increase the peptide stability.

CONCLUSIONS

To explore the effect of fatty acid length on the stability and anticancer activity of antimicrobial peptide F1, eight lipopeptides were synthesized by modification with fatty acids. Compared with F1, A-10 has better serum and proteinase K stability. We found that after fatty acid modification, A-10 can self-assemble to enhance its stability. In terms of biological activity, A-10 has better activity against cancer cells. In addition, the LDH leakage assay and flow cytometry results showed that A-10 not only destroyed the cell membrane but also promoted apoptosis; moreover, A-10 arrested cells in the G0/G1 phase. Fatty acid modification increases the ability of the peptide to destroy cells, which can improve the killing effect. However, the hemolytic activity of A-10 was not significantly improved compared to F1. In summary, although the exact mechanism of these lipopeptides needs further study, our work confirmed that fatty acid modification can effectively enhance the anticancer activity of Figainin 1. The selection of appropriate fatty acids for structural modification is necessary to improve the anticancer activity of antimicrobial peptides.

MATERIALS AND METHODS

Materials. All Fmoc amino acids and *N*,*N*′-diisopropylcarbodiimide (DIC), 1-hydroxybenzotriazol (HOBT), triisopropylsilane (TIS), *N*,*N*-diisopropylethylamine (DIEA), and trifluoroacetic acid (TFA) were purchased from Energy Chemical (Shanghai, China). *N*,*N*-Dimethylformamide (DMF) and dichloromethane (DCM) were purchased from Titan Technology. Rink amide AM resin was obtained from Sunresin (Xi'an, China). The Caspase 3, Proteinase K, Cell Counting Kit-8, LDH cytotoxicity, Cell Cycle and Apoptosis, and Reactive Oxygen Species assay kits, and Triton X-100 were purchased from Beyotime.

The human breast cancer cell line (MCF-7), human colon cell line (HCT-116), human lung cell line (A549), human chronic myeloid leukemia cell line (K562), and human acute lymphoblastic leukemia cell line (CCRF-CEM) were obtained from Huibai Biotechnology (Shenyang, China). Minimum essential medium (MEM), RPMI 1640, Iscove's modified Dulbecco's medium (IMDM), and fetal bovine serum (FBS) were purchased from Huibai Biotechnology (Shenyang, China).

Peptide Synthesis. All peptides were synthesized by using the standard Fmoc solid-phase synthesis strategy on a Rink amide-AM resin (0.33 mmol/g). The *N*-Fmoc group of the resin was removed with 20% piperidine/DMF (30 min at room temperature), and the resin was then coupled with 4 equiv of N^{α}-protected amino acid in the presence of DIC (4 equiv) and HOBt (4 equiv) at room temperature for 3 h. After each Fmoc removal or coupling, the resin was washed three times with dimethylformamide (DMF) and three times with CH_2Cl_2 for 3 min each time. After the final deprotection, the amino terminus was treated with fatty acid (4 equiv), DIC (4 equiv), and HOBt (4 equiv) at room temperature for 3 h. Peptides were cleaved using TFA/1,2-ethanedithiol/triisopropylsilane/H_2O (90/5/3/2 (v/v)) for 2 h of reaction and precipitated in cold diethyl ether.

The crude peptides were purified and identified by HPLC and high-resolution mass spectrometry (HRMS), respectively. The purity of each of the peptides was above 95%, as confirmed by HPLC.

RP-HPLC Analysis. Peptide samples were analyzed on a Waters 1525 HPLC using an Agilent ZORBAX column (4.6 × 250 mm^2, 5 μm) with linear A/B gradient elution at 25 °C. Solvent A was 0.1% TFA in H_2O, and solvent B was 0.1% TFA in 100% MeOH. For peptide runs, the linear gradient was performed for 20 min as follows: the initial conditions were 50% solvent A and 50% solvent B, changing to 0% solvent A and 100% solvent B over 10 min at a flow rate of 1 mL/min, and keep 0% solvent A and 100% solvent B to 20 min. Signals were detected at an altitude of 210 nm.

Cell Culture. All of the cell lines used in the experiments were cultured at 37 °C under a humidified atmosphere containing 5% CO_2. MCF-7 cells were maintained in MEM with 10% FBS. HCT-116 cells, CCRF-CEM cells, and A549 cells were maintained in RPMI 1640 with 10% FBS. K562 cells were maintained in IMDM with 10% FBS. All of the media used in the experiments were supplemented with 100 μg/mL streptomycin and 100 U/mL penicillin.

Cell Viability Assays. MCF-7 cells, HCT-116 cells, and A549 cells were seeded at a density of 5 × 10^3 cells per well in a 96-well plate. After 24 h, the culture medium was removed, and another 100 μL of MEM or RPMI 1640 containing various concentrations of peptides was added to the wells. The effects of the peptides on cell viability were determined using the CCK-8 assay after the cells were incubated at 37 °C for 24 h. K562 cells and CCRF-CEM cells were seeded at a density of 5 × 10^3 cells per well in a 96-well plate. After 24 h, another 100 μL of IMDM or RPMI 1640 containing various concentrations of peptides was added to the wells. The effects of the peptides on cell viability were determined using the CCK-8 assay after the cells were incubated at 37 °C for 24 h. IC_{50} values were calculated using GraphPad Prism 9.

https://doi.org/10.1021/acsomega.3c06806
ACS Omega 2023, 8, 41876−41884

CD Spectroscopy. The CD spectra of the peptides were recorded on a Biologic MOS-450 CD spectrometer in the wavelength range of 190−260 nm. Peptides (50 μM) were dissolved in 50% (v/v) TFE/PBS or PBS. CD spectral measurements were taken in a quartz cuvette with a path length of 0.1 cm at room temperature. The relative helicity of each peptide was estimated using a previous method.

Peptide Self-Assembly Assays. The self-assembly propensity of the peptides was detected with the 1,8-ANS binding experiment according to a reported method. Briefly, 150 μL of PBS containing peptides with concentrations ranging from 1 to 50 μM was added to 0.5 mL centrifuge tubes containing ANS at a final concentration of 40 μM. The mixed solutions were vortexed for 5 min. Finally, 100 μL of the sample solution was added to a 96-well plate, and the fluorescence emission intensity was measured using a microplate reader. The excitation and emission wavelengths were 330 and 492 nm, respectively.

Hemolysis Assay. Red blood cells were collected from mice and resuspended in PBS to a concentration of 4% (V/V). 100 μL of the suspension was added to a 96-well plate, and then 100 μL of peptide solution with a concentration ranging from 1 to 50 μM was added. PBS and 0.1% Triton X-100 were used as controls for 0 and 100% hemolysis, respectively. After incubation for 1 h, the cells were centrifuged at 1000*g* for 10 min. A 100 μL sample of the supernatant was transferred to a fresh 96-well plate, and the amount of released hemoglobin was evaluated at 450 nm by using a microplate reader.

Cell Cycle Analysis. According to the manufacturer's instructions for the Cell Cycle and Apoptosis Analysis Kit (Beyotime, Shanghai, China), cell cycle analysis in K562 cells was performed. K562 cells were seeded at 5×10^6 cells/well in 6-well plate 24 h before treatment. After treatment with 10 μM peptides for 24 h, the cells were fixed and stained with the PI/RNase staining solution. Cell cycle analysis was performed with flow cytometry.

Determination of Reactive Oxygen Species (ROS) Production. According to the manufacturer's instructions for the Reactive Oxygen Species Assay Kit (Beyotime, Shanghai, China), reactive oxygen species production in K562 cells was assessed. K562 cells were seeded at 5×10^6 cells/well in six-well plates 24 h before treatment. After treatment with 10 μM peptides or Rosup for 24 h, the cells were treated with 20 μM DCFH-DA for 20 min. After incubation, the cells were washed with PBS, and reactive oxygen species production was detected by flow cytometry.

LDH Leakage Assays. The LDH release assay was used to determine the membrane integrity using the Cytotoxicity Detection Kit (Beyotime, China). The LDH assay was completed according to the manufacturer's instructions. Briefly, K562 cells were seeded in a 96-well plate for 24 h. Then, 100 μL of serum-free medium containing various concentrations of peptides and LDH release reagent was added for 24 h of incubation. Next, the cell culture plate was centrifuged at 400*g* for 5 min in a multiwell plate centrifuge. Then, 120 μL of the supernatant from each well was added to the corresponding well of a new 96-well plate. Afterward, 60 μL of LDH detection working solution was added to each well. The samples were incubated on a shaker at room temperature for 30 min. Neither peptides nor the LDH-releasing reagent was added to the control, which was taken as no leakage. The fluorescence was detected at 490 nm using a microplate reader. The cells treated with the LDH-releasing reagent represented 100% leakage (total LDH release).

Flow Cytometry Assay. We used an Annexin V-FITC/PI apoptosis detection kit (Beyotime, China) to detect apoptotic K562 cells. The LDH assay was completed according to the manufacturer's instructions. Briefly, 5×10^6/mL cells were plated in six-well plates in medium and incubated with 10 μM peptides. After 24 h of incubation, the cells were collected and washed with PBS. Then, the cells were suspended in Annexin V binding buffer, and Annexin V-FITC solution and PI were added for 10 min of incubation at room temperature in the dark. The stained cells were analyzed by flow cytometry at an emission wavelength of 525 nm for FITC and an emission wavelength of 620 nm for PI signal detection. Annexin V−/PI− indicates live cells, Annexin V+/PI− indicates early apoptotic cells, Annexin V+/PI+ indicates late apoptotic cells and necrotic cells, and Annexin V−/PI+ indicates necrotic cells.

Serum Stability Assay. The serum stabilities of the peptides were determined, as previously described. Each peptide solution (10 mM) was incubated with 10% serum at 37 °C for 0, 1, 5, 10, and 24 h. Then, H_2O/ACN (60:40 v/v) with 1% TFA was added to the serum. The cloudy mixture was centrifuged at 12 000 rpm for 3 min. The supernatant was analyzed by RP-HPLC. The analytical method utilized gradient elution from 10 to 100% MeOH/H_2O (containing 0.1% TFA) over 30 min at a flow rate of 1 mL/min.

Proteinase K Stability Assay. The Proteinase K stabilities of the peptides were determined as previously described. Each peptide solution (10 mM) was incubated with Proteinase K at 37 °C for 0, 1, 5, 10, and 24 h. Then, H_2O/ACN (60:40 v/v) with 1% TFA was added to the mixed solution. The cloudy mixture was centrifuged at 12 000 rpm for 3 min. The supernatant was analyzed by RP-HPLC. The analytical method utilized gradient elution from 10 to 100% MeOH/H_2O (containing 0.1% TFA) over 30 min at a flow rate of 1 mL/min.

■ ASSOCIATED CONTENT

Supporting Information

The Supporting Information is available free of charge at https://pubs.acs.org/doi/10.1021/acsomega.3c06806.

Circular dichroism analysis (Figure S1); hemolytic activity assay (Figure S2); and ESI mass spectra and analytical reversed-phase HPLC chromatogram for purified peptides (Figures S3−S11) (PDF)

■ AUTHOR INFORMATION

Corresponding Authors

Huali Yang − *Key Laboratory of Structure-Based Drug Design & Discovery, Ministry of Education, School of Pharmaceutical Engineering, Shenyang Pharmaceutical University, Shenyang 110016, China*; Email: yanghl@syphu.edu.cn

Yang Liu − *Key Laboratory of Structure-Based Drug Design & Discovery, Ministry of Education, School of Pharmaceutical Engineering, Shenyang Pharmaceutical University, Shenyang 110016, China*; orcid.org/0000-0002-9284-1944; Email: y.liu@syphu.edu.cn

https://doi.org/10.1021/acsomega.3c06806
ACS Omega 2023, 8, 41876−41884

Authors

Zhenbin Han − *Key Laboratory of Structure-Based Drug Design & Discovery, Ministry of Education, School of Pharmaceutical Engineering, Shenyang Pharmaceutical University, Shenyang 110016, China*

Dongmei Feng − *Key Laboratory of Structure-Based Drug Design & Discovery, Ministry of Education, School of Pharmaceutical Engineering, Shenyang Pharmaceutical University, Shenyang 110016, China*

Wenxuan Wang − *Key Laboratory of Structure-Based Drug Design & Discovery, Ministry of Education, School of Pharmaceutical Engineering, Shenyang Pharmaceutical University, Shenyang 110016, China*

Yue Wang − *Key Laboratory of Structure-Based Drug Design & Discovery, Ministry of Education, School of Pharmaceutical Engineering, Shenyang Pharmaceutical University, Shenyang 110016, China*

Maosheng Cheng − *Key Laboratory of Structure-Based Drug Design & Discovery, Ministry of Education, School of Pharmaceutical Engineering, Shenyang Pharmaceutical University, Shenyang 110016, China;* orcid.org/0000-0001-9073-4806

Complete contact information is available at: https://pubs.acs.org/10.1021/acsomega.3c06806

Author Contributions

Z.H. and D.F. carried out the experiments and performed data analysis. W.W. and Y.W. participated in part of the experiments. Z.H. prepared the manuscript, and Y.L. revised the manuscript. M.C., H.Y., and Y.L. supervised and financially supported the project. All of the authors have read and approved the final manuscript.

Notes

The authors declare no competing financial interest.

■ ACKNOWLEDGMENTS

This work was financially supported by the National Natural Science Foundation of China (22177079) and the Program for Liaoning Innovative Talents in University (LR2017043).

■ ABBREVIATIONS

F1, figainin 1; CML, chronic myelogenous leukemia; TFE, trifluoroethanol; CCK8, cell counting kit-8; LDH, lactate dehydrogenase; ROS, reactive oxygen species; ANS, 8-anilino-1-naphthalenesulfonate; HRMS, high-resolution mass spectrometry; DIC, *N,N′*-diisopropylcarbodiimide; HOBT, 1-hydroxybenzotriazol; TIS, triisopropylsilane; DIEA, *N,N*-diisopropylethylamine; TFA, trifluoroacetic acid; DMF, *N,N*-dimethylformamide; DCM, dichloromethane; MEM, minimum essential medium; IMDM, Iscove's modified Dulbecco's medium; FBS, fetal bovine serum

■ REFERENCES

(1) Siegel, R. L.; Miller, K. D.; Wagle, N. S.; Jemal, A. Cancer statistics, 2023. *CA, Cancer J. Clin.* **2023**, *73* (1), 17−48.

(2) Osman, A. E. G.; Deininger, M. W. Chronic Myeloid Leukemia: Modern therapies, current challenges and future directions. *Blood Rev.* **2021**, *49*, No. 100825, DOI: 10.1016/j.blre.2021.100825.

(3) Kantarjian, H. M.; Jain, N.; Garcia-Manero, G.; Welch, M. A.; Ravandi, F.; Wierda, W. G.; Jabbour, E. J. The cure of leukemia through the optimizt's prism. *Cancer* **2022**, *128* (2), 240−259.

(4) Pan, Y. L.; Zeng, S. X.; Hao, R. R.; Liang, M. H.; Shen, Z. R.; Huang, W. H. The progress of small-molecules and degraders against BCR-ABL for the treatment of CML. *Eur. J. Med. Chem.* **2022**, *238*, No. 114442.

(5) García-Gutiérrez, V.; Breccia, M.; Jabbour, E.; Mauro, M.; Cortes, J. E. A clinician perspective on the treatment of chronic myeloid leukemia in the chronic phase. *J. Hematol. Oncol.* **2022**, *15* (1), 90.

(6) Sundaram, D. N. M.; Jiang, X.; Brandwein, J. M.; Valencia-Serna, J.; Remant, K. C.; Uludag, H. Current outlook on drug resistance in chronic myeloid leukemia (CML) and potential therapeutic options. *Drug Discovery Today* **2019**, *24* (7), 1355−1369.

(7) Ghaly, G.; Tallima, H.; Dabbish, E.; Badr El-Din, N.; Abd El-Rahman, M. K.; Ibrahim, M. A. A.; Shoeib, T. Anti-Cancer Peptides: Status and Future Prospects. *Molecules* **2023**, *28* (3), No. 1148, DOI: 10.3390/molecules28031148.

(8) Kurrikoff, K.; Aphkhazava, D.; Langel, U. The future of peptides in cancer treatment. *Curr. Opin. Pharmacol.* **2019**, *47*, 27−32.

(9) Xu, X.; Lai, R. The chemistry and biological activities of peptides from amphibian skin secretions. *Chem. Rev.* **2015**, *115* (4), 1760−1846.

(10) Wang, G.; Li, X.; Wang, Z. APD3: the antimicrobial peptide database as a tool for research and education. *Nucleic Acids Res.* **2016**, *44* (1), D1087−D1093.

(11) Huang, Y.; Feng, Q.; Yan, Q.; Hao, X.; Chen, Y. Alpha-Helical Cationic Anticancer Peptides: A Promising Candidate for Novel Anticancer Drugs. *Mini-Rev. Med. Chem.* **2015**, *15* (1), 73−81.

(12) Brunetti, A. E.; Fuzo, C. A.; Aguilar, S.; Rivera-Correa, M.; Marani, M. M.; Lopes, N. P. The Significance of Hypervariability and Conserved Motifs in Antimicrobial Peptides from Tree Frogs. *J. Nat. Prod.* **2023**, *86* (7), 1761−1769.

(13) Aguilar, S.; Brunetti, A. E.; Garay, A. V.; Santos, L. C.; Perez, L. O.; Moreira, D.; Cancelarich, N. L.; Barbosa, E. A.; Basso, N. G.; de Freitas, S. M.; Faivovich, J.; Brand, G.; Cabrera, G. M.; Leite, J.; Marani, M. M. Structure and function of cationic hylin bioactive peptides from the tree frog Boana pulchella in interaction with lipid membranes. *Peptides* **2023**, *159*, No. 170900.

(14) de Freitas, G. G.; Barbosa, J. M.; Santana, C. J. C.; Magalhaes, A. C. M.; Macedo, K. W. R.; Souza, J. O.; Castro, J. S.; Vasconcelos, I. A.; Souza, A. A.; Freitas, S. M.; Bao, S. N.; Costa, S. R.; Brand, G. D.; Chaves, I. M.; Costa, V. V.; Fontes, W.; Pires Junior, O. R.; Castro, M. S. Purification and Biological Properties of Raniseptins-3 and −6, Two Antimicrobial Peptides from Boana raniceps (Cope, 1862) Skin Secretion. *Biomolecules* **2023**, *13* (3), No. 576, DOI: 10.3390/biom13030576.

(15) Muniz, G. S. V.; Duarte, E. L.; Lorenzon, E. N.; Cilli, E. M.; Lamy, M. T. What different physical techniques can disclose about disruptions on membrane structure caused by the antimicrobial peptide Hylin a1 and a more positively charged analogue. *Chem. Phys. Lipids* **2022**, *243*, No. 105173.

(16) Zhang, R.; Xu, L.; Dong, C. Antimicrobial Peptides: An Overview of their Structure, Function and Mechanism of Action. *Protein Pept. Lett.* **2022**, *29* (8), 641−650.

(17) Nugrahadi, P. P.; Hinrichs, W. L. J.; Frijlink, H. W.; Schoneich, C.; Avanti, C. Designing Formulation Strategies for Enhanced Stability of Therapeutic Peptides in Aqueous Solutions: A Review. *Pharmaceutics* **2023**, *15* (3), No. 935, DOI: 10.3390/pharmaceutics15030935.

(18) Lai, Z.; Yuan, X.; Chen, H.; Zhu, Y.; Dong, N.; Shan, A. Strategies employed in the design of antimicrobial peptides with enhanced proteolytic stability. *Biotechnol. Adv.* **2022**, *59*, No. 107962.

(19) Fetse, J.; Kandel, S.; Mamani, U.-F.; Cheng, K. Recent advances in the development of therapeutic peptides. *Trends Pharmacol. Sci.* **2023**, *44* (7), 425−441.

(20) Zhang, C.; Yang, X.; Meng, X.; Wu, L.; Liu, X.; Gao, J.; Liu, S.; Wu, J.; Huang, D.; Wang, Z.; Su, X. Discovery of Novel PTP1B Inhibitors with Once-Weekly Therapeutic Potential for Type 2 Diabetes: Design, Synthesis, and In Vitro and In Vivo Investigations of BimBH3 Peptide Analogues. *J. Med. Chem.* **2023**, *66* (4), 3030−3044.

(21) Ma, L.; Huang, S.; Xie, H.; Ma, P.; Jia, B.; Yao, Y.; Gao, Y.; Li, W.; Song, J.; Zhang, W. Influence of chain length on the anticancer activity of the antimicrobial peptide CAMEL with fatty acid modification. *Eur. J. Med. Chem.* **2022**, *239*, No. 114557.
(22) Jian, C.; Zhang, P.; Ma, J.; Jian, S.; Zhang, Q.; Liu, B.; Liang, S.; Liu, M.; Zeng, Y.; Liu, Z. The Roles of Fatty-Acid Modification in the Activity of the Anticancer Peptide R-Lycosin-I. *Mol. Pharmaceutics* **2018**, *15* (10), 4612−4620.
(23) Yang, Y.; Zhang, H.; Wanyan, Y.; Liu, K.; Lv, T.; Li, M.; Chen, Y. Effect of Hydrophobicity on the Anticancer Activity of Fatty-Acyl-Conjugated CM4 in Breast Cancer Cells. *ACS Omega* **2020**, *5* (34), 21513−21523.
(24) Chang, L.; Wu, X.; Ran, K.; Tian, Y.; Ouyang, X.; Liu, H.; Gou, S.; Zhang, Y.; Ni, J. One New Acid-Activated Hybrid Anticancer Peptide by Coupling with a Desirable pH-Sensitive Anionic Partner Peptide. *ACS Omega* **2023**, *8* (8), 7536−7545.
(25) Zhang, P.; Jian, C.; Jian, S.; Zhang, Q.; Sun, X.; Nie, L.; Liu, B.; Li, F.; Li, J.; Liu, M.; Liang, S.; Zeng, Y.; Liu, Z. Position Effect of Fatty Acid Modification on the Cytotoxicity and Antimetastasis Potential of the Cytotoxic Peptide Lycosin-I. *J. Med. Chem.* **2019**, *62* (24), 11108−11118.
(26) Mangoni, M. L.; Casciaro, B. Development of Antimicrobial Peptides from Amphibians. *Antibiotics* **2020**, *9* (11), No. 772, DOI: 10.3390/antibiotics9110772.
(27) Santana, C. J. C.; Magalhaes, A. C. M.; Dos Santos Junior, A. C. M.; Ricart, C. A. O.; Lima, B. D.; Alvares, A.; Freitas, S. M.; Pires, O. R., Jr.; Fontes, W.; Castro, M. S. Figainin 1, a Novel Amphibian Skin Peptide with Antimicrobial and Antiproliferative Properties. *Antibiotics* **2020**, *9* (9), No. 625, DOI: 10.3390/antibiotics9090625.
(28) Selvaraj, S. P.; Chen, J. Y. Conjugation of antimicrobial peptides to enhance therapeutic efficacy. *Eur. J. Med. Chem.* **2023**, *259*, No. 115680.
(29) Bhat, M.; Jatyan, R.; Mittal, A.; Mahato, R. I.; Chitkara, D. Opportunities and challenges of fatty acid conjugated therapeutics. *Chem. Phys. Lipids* **2021**, *236*, No. 105053.
(30) Chu-Kung, A. F.; Nguyen, R.; Bozzelli, K. N.; Tirrell, M. Chain length dependence of antimicrobial peptide-fatty acid conjugate activity. *J. Colloid Interface Sci.* **2010**, *345* (2), 160−167.
(31) Oh, H. S.; Kim, S.; Cho, H.; Lee, K. H. Development of novel lipid-peptide hybrid compounds with antibacterial activity from natural cationic antibacterial peptides. *Bioorg. Med. Chem. Lett.* **2004**, *14* (5), 1109−1113.
(32) Nasompag, S.; Dechsiri, P.; Hongsing, N.; Phonimdaeng, P.; Daduang, S.; Klaynongsruang, S.; Camesano, T. A.; Patramanon, R. Effect of acyl chain length on therapeutic activity and mode of action of the CX-KYR-NH2 antimicrobial lipopeptide. *Biochim. Biophys. Acta* **2015**, *1848* (10), 2351−2364.
(33) Gabernet, G.; Müller, A. T.; Hiss, J. A.; Schneider, G. Membranolytic anticancer peptides. *MedChemComm* **2016**, *7* (12), 2232−2245.
(34) Klein, R.; Nagy, O.; Tothova, C.; Chovanova, F. Clinical and Diagnostic Significance of Lactate Dehydrogenase and Its Isoenzymes in Animals. *Vet. Med. Int.* **2020**, *2020*, No. 5346483.
(35) Zhou, Y.; Qi, M.; Yang, M. Current Status and Future Perspectives of Lactate Dehydrogenase Detection and Medical Implications: A Review. *Biosensors* **2022**, *12* (12), No. 1145, DOI: 10.3390/bios12121145.
(36) Forkasiewicz, A.; Dorociak, M.; Stach, K.; Szelachowski, P.; Tabola, R.; Augoff, K. The usefulness of lactate dehydrogenase measurements in current oncological practice. *Cell. Mol. Biol. Lett.* **2020**, *25*, 35.
(37) Zhu, L. N.; Fu, C. Y.; Zhang, S. F.; Chen, W.; Jin, Y. T.; Zhao, F. K. Novel cytotoxic exhibition mode of antimicrobial peptide anoplin in MEL cells, the cell line of murine Friend leukemia virus-induced leukemic cells. *J. Pept. Sci.* **2013**, *19* (9), 566−574.
(38) Paredes-Gamero, E. J.; Martins, M. N.; Cappabianco, F. A.; Ide, J. S.; Miranda, A. Characterization of dual effects induced by antimicrobial peptides: regulated cell death or membrane disruption. *Biochim. Biophys. Acta* **2012**, *1820* (7), 1062−1072.
(39) Ju, X.; Fan, D.; Kong, L.; Yang, Q.; Zhu, Y.; Zhang, S.; Su, G.; Li, Y. Antimicrobial Peptide Brevinin-1RL1 from Frog Skin Secretion Induces Apoptosis and Necrosis of Tumor Cells. *Molecules* **2021**, *26* (7), No. 2059, DOI: 10.3390/molecules26072059.
(40) Bhola, P. D.; Letai, A. Mitochondria-Judges and Executioners of Cell Death Sentences. *Mol. Cell* **2016**, *61* (5), 695−704.
(41) Diaz-Moralli, S.; Tarrado-Castellarnau, M.; Miranda, A.; Cascante, M. Targeting cell cycle regulation in cancer therapy. *Pharmacol. Ther.* **2013**, *138* (2), 255−271.
(42) Zhong, C.; Liu, T.; Gou, S.; He, Y.; Zhu, N.; Zhu, Y.; Wang, L.; Liu, H.; Zhang, Y.; Yao, J.; Ni, J. Design and synthesis of new N-terminal fatty acid modified-antimicrobial peptide analogues with potent in vitro biological activity. *Eur. J. Med. Chem.* **2019**, *182*, No. 111636.

https://doi.org/10.1021/acsomega.3c06806
ACS Omega 2023, 8, 41876−41884